DESIGN OF HIGH CAPACITY 3D PRINT CODES AIMING FOR ROBUSTNESS TO THE PS CHANNEL AND EXTERNAL DISTORTIONS

Joceli Mayer[a], *J.C.M. Bermudez*[a],

A. P. Legg[b], *B. F. Uchôa-Filho*[b*]

LPDS[a] and GPqCom[b] Laboratories - EEL
Federal University of Santa Catarina - UFSC
Florianopolis SC, Brazil

D. Mukherjee[1], *A. Said*[1], *R. Samadani*[1],

S. Simske[2†]

Hewlett Packard Laboratories
Palo Alto CA[1], Fort Collins CO[2], USA

ABSTRACT

The process of adding high-density information onto printed material enables and improves interesting hardcopy document applications, such as: security, authentication, physical-electronic round tripping, item-level tagging as well as consumer/product interaction. This investigation on robust and high capacity print codes aims to maximize information payload in a given printed page area, subject to robustness to distortions originated by printing and scanning processes and also to degradations introduced by user manipulation of printed documents. The novel approach includes statistical print-and-scan channel characterization, designing of robust segmentation, unsupervised Bayesian color classification with expectation-maximization algorithm for parameters estimation of a mixture of Gaussians model and design of error correction codes. Results illustrate the performance evaluated under real channel and distortions conditions. High payload is achieved with sufficient robustness to distortions resulting of regular office hardcopy document handling: print-and-scan channel and user manipulation.

Index Terms— Statistical pattern classification, hardcopy watermarking, document authentication.

1. INTRODUCTION

Researchers have recently shown enormous interest in investigating high-capacity two-dimensional color print patterns codes also termed as "3D barcodes" since including colors adds a third dimension to the 2D patterns. Several novel applications require relatively large amounts of information to be transmitted using printed paper. Such applications require robustness to inevitable distortions in the printing and scanning processes as well as to various external degradations. Most prior work on printed codes is restricted to 1D barcodes that have limited payload. A recent investigation [1] has shown a great potential of two-dimensional printed code technologies to improve information transmission using paper. High-capacity printed barcodes provide new value for prints by improving security, print repurposability and supplemental information transmission. Related research on barcodes aimed to be captured by cell phones or consumer digital cameras has been proposed in the literature [2, 3, 4] and some results can be applied to our research that involves acquisition by scanners. Recent studies such as [1, 5, 6] investigate the use of 2D patterns to improve capacity and robustness. The literature points out that significant improvements in capacity and robustness can be achieved by exploiting color and 2D patterns. Achieving robust high-capacity information transmission over the print-and-scan channel requires addressing of a variety of degradations. These include distortions due to: i) Noise and the optical blurring in the channel; ii) Geometric disturbances; iii) Ink fading, spills, creases and aging; iv) Document manipulation by the user. Novel error correction coding, statistical classification and robust segmentation techniques need to be investigated to address these distortions. Another challenge is to develop technologies that are robust enough for general purpose use over a variety of embedding (printing) and detection (scanning) devices. By interacting with the paper using 2D color codes, new and interesting applications will be possible. Some examples include the restoration of aged printed photos with the help of 2D color codes printed on the back of the photo [7], content authentication using barcodes confined to small areas, security printing with smart labels [8, 9], and deterrents for branded product counterfeiting. This paper reports recent results of an ongoing research effort to improve algorithms operating with 2D color patterns to achieve higher capacity and robustness for novel applications demanding high information density by printed area of the paper.

2. COMMUNICATION CHANNEL

The information is embedded into the color print codes and sent through the communication channel as illustrated in Figure 1.

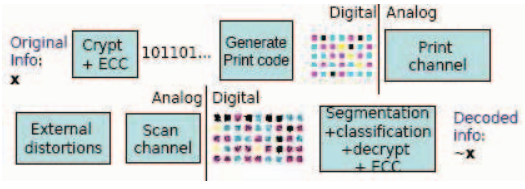

Fig. 1: Information embedding, communication channel and information decoding system.

The communication channel includes the print-and-scan channel (PS) and external distortions. The PS channel includes linear and non-linear distortions: electronic, ink and paper noise; optical and motion blurring in the scanner device, ink print spreading and

*E-mails: {mayer,bermudez,andrei,uchoa}@eel.ufsc.br.
†E-mails: {Debargha.Mukherjee, Amir.Said, Ramin.Samadani, Steven.Simske}@hp.com.

geometrical disturbances. A detailed description of these distortions for monochromatic PS channel is provided in [10]. External distortions occur due to normal user manipulation as a result of coffee spills, pen/pencil scribing, fingerprints and due to ink and paper aging. These degradations are illustrated in Figures 2 and 3 for the HP C4280 inkjet printer/scanner device.

Fig. 2: Distortions in the PS channel.

Fig. 3: External distortions due to pen scribing and coffee spills.

3. COLOR CHARACTERIZATION

The scanning acquisition system provides a triplet {R,G,B} of values in the RGB color system for each scanned pixel sample. Since most consumer printing devices employ the CMYK print system with four ink colors (cyan, magenta, yellow and black), the CMY color system is preferred to represent the acquired samples. Given its RGB representation, each pixel can be alternatively represented as a 3-dimensional sample $\boldsymbol{x} = [1-R \;\; 1-G \;\; 1-B]^T = [C \;\; M \;\; Y]^T$. The digital print code employs CMYK ink colors, which slightly deviates from pure CMYK colors. Moreover, the PS channel introduces color spreading for each pixel. The resulting spreading of the samples is illustrated in the CMY cube in Figure 4(a) for the HP C4280 inkjet printer/scanner device. The optical and mechanical blurring and the electronic noise generated by the scanner device contributes significantly to the resulting color spreading as observed in the experiments. Thus, similar spreading occurs either with inkjets or laser printers.

The color classification task can be facilitated if the sample mean of the pixels within a block pattern is used to represent that block. This results in considerable reduction of color spreading for each block within the CMY cube, as illustrated at Fig. 4(b). Notice that reduced spreading improves the classification accuracy.

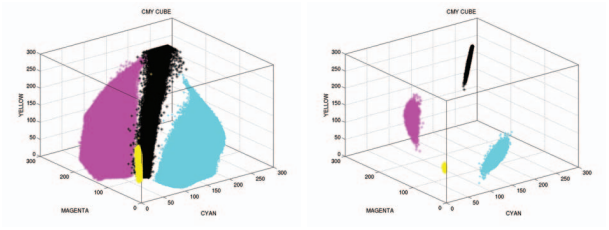

(a) (b)

Fig. 4: (a) Individual samples color spreading. (b) Block sample means color spreading due to the PS channel.

4. STATISTICAL COLOR CLASSIFICATION

Color classification is an important step in the information recovery process. In this work we employ a Bayesian approach [11] to classify each printed and scanned block pattern in one of the C, M, Y or K classes. A feature vector $\boldsymbol{y}_j = f(\boldsymbol{x} \in B_j)$ is extracted from the acquired 3-dimensional samples within the j-th block pattern B_j. $\boldsymbol{y}_j$ is a D-dimensional vector which is a function of the samples within B_j. Consider the class conditional probability density function (pdf), $p(\boldsymbol{y}|\omega_i)$, of the feature vectors $\boldsymbol{y}$ belonging to class ω_i, where ω_1: cyan, ω_2: magenta, ω_3: yellow, ω_4: black. Define $P(\omega_i)$, $i = 1, \ldots, 4$ as the prior probability. Thus, the posterior class probabilities are given by [11]

$$P(\omega_i|\boldsymbol{y}) = \frac{p(\boldsymbol{y}|\omega_i)P(\omega_i)}{\sum_{j=1}^{4} p(\boldsymbol{y}|\omega_j)P(\omega_j)}. \tag{1}$$

The posteriors provide information about which is the most probable embedded color for a given pattern block. In this work we build each feature vector using the sample mean and the average hue color (AVGH) [12] of the samples in the block. This leads to a 4-dimensional feature vector $\boldsymbol{y} = [\frac{1}{M}\sum_{j=1}^{M} \boldsymbol{x}_j; \quad AVGH]$. As all elements in $\boldsymbol{y}$ are sample averages of a large number of samples, we invoke Central Limit Theorem [11] and model the conditional pdfs of $\boldsymbol{y}$ as Gaussian. Thus, the class conditional probability density function for a given class ω_i is given by:

$$p(\boldsymbol{y}|\omega_i) = \frac{1}{(2\pi)^{3/2}|\boldsymbol{C}_i|^{1/2}} \exp\Big\{-\frac{1}{2}(\boldsymbol{y}-\boldsymbol{\mu}_i)^T \boldsymbol{C}_i^{-1}(\boldsymbol{y}-\boldsymbol{\mu}_i)\Big\} \tag{2}$$

The covariance matrices, $\boldsymbol{C}_i$, the mean vectors, $\boldsymbol{\mu}_i$ and the prior probabilities $P(\omega_i)$, $i = 1, \ldots, 4$ need to be estimated given the observed print codes. This issue is addressed in the next section by modeling the received printed codes as a mixture of Gaussians.

5. ESTIMATING THE DENSITY PARAMETERS

The density parameters can be estimated by either supervised or unsupervised training. The supervised training would require using reference blocks with previously defined known colors or accessing the original printing device. The chosen unsupervised estimation approach does not require reference blocks or accessing the device.

Assuming that data is distributed according to a mixture of K Gaussians,

$$p(\boldsymbol{y}) = \sum_{k=1}^{K} P(\omega_k) \frac{1}{(2\pi)^{D/2}\,|\boldsymbol{C}_k|^{\frac{1}{2}}} e^{-\frac{1}{2}(\boldsymbol{y}-\boldsymbol{\mu}_k)^T \boldsymbol{C}_k^{-1}(\boldsymbol{y}-\boldsymbol{\mu}_k)} \tag{3}$$

the problem at hand is to estimate which parameters should be used for the mixture of $K = 4$ Gaussians (4 colors or classes). The number of descriptors chosen is $D = 4$, where the first 3 components represent the average sample mean inside of a block, namely, average of the cyan, magenta and yellow components. The 4th component was chosen to be the average color hue of the block samples where color hue represents the angle in the HSV color model [12].

We propose to employ the **Expectation-Maximization** (EM) algorithm [11] to estimate the parameters of (3). The algorithm initially estimates the mean vector parameter using the K-means clustering and then estimates the initial covariance matrices using the closest patterns to the estimated mean vector. Later, it iterates between evaluating the expectation of $\boldsymbol{y}$ for each Gaussian density and the maximization of new parameters considering the computed expectations. The algorithm stops when the variation on the parameters is smaller than a predefined value.

The four posteriors are computed using the estimated parameters. The color embedded at block B_j is classified in the class i that results in the greatest $P(\omega_i|\boldsymbol{y})$. In the absence of user induced degradations, the unsupervised estimation with EM and Bayesian classification provides an optimal framework to deal with print and scan channel disturbances. In the next section, Error Correction Codes (ECC) are proposed to deal with external noises that may not follow the assumed distribution for the received print codes.

6. ERROR CORRECTION CODE

The external distortions introduced by coffee spills and pen scribing, for instance, are not properly modeled by Gaussian pdf and thus need to be dealt with an external error correction mechanism. The proper tradeoff between code robustness and code rate depends on the typical external errors found by the intended applications. A size of about one quarter (4 inches by 4 inches area) of document page is defined for the print codes. Each print code is designed with a size of 5 by 5 pixels square block using a unique color (C,M, Y or K) and with a separating gap of 5 white pixels among print codes. This setup can be properly changed upon the application requirements. The experiments indicated that typical external errors are confined within about 0.25% of the print codes area. With this scenario in mind, the error correction codes are designed to provide a robustness to spill coffee and pen scribing distortions with area no larger than 0.5% of the print codes area and the code redundancy is less than 20% of the message, resulting in a code rate larger than 0.82. Both standard Bose, Chaudhuri, and Hocquenghem (BCH) and the Reed-Solomon (RS) codes with hard decision [13] are designed to provide the aforementioned specifications.

The print codes consist of a square of 240 by 240 colored square blocks as illustrated in the figures. It corresponds to a sequence of 240 by 240 = 57,600 blocks $\rightarrow$ 57,600 $\times$ 2 bits per colored block = 115,200 bits. The BCH codeword length is n = 511 bits, information word length is k = 421 bits, and a correction capacity of t = 10 bits per word is chosen. A bit "0" is appended at the end of each codeword, making the codeword length a power of 2. The print codes consists of a sequence of 115,200/512 = 225 binary codewords, comprising 225 $\times$ 421 = 94,725 information bits. For the RS code a similar approach is taken resulting in a higher correction capacity using n= 511, k = 423, t = 44 and 115,200/512 $\times$ 423 = 95,175 information bits per print codes using up 4 inches by 4 inches area.

7. SEGMENTATION

The segmentation requires the localization and pattern segmentation of the color print codes. The overall system performance is highly dependent on these tasks [2]. They are required prior to the color classification and to the decoding by the ECC algorithm. Different segmentation approaches can be employed provided that some complicating issues are properly addressed, including: non-uniform illumination of the scanning device, geometric distortions introduced by printing mechanics/heating and scanning alignment, proprietary scanner optical system and associated optical distortions, paper texture and imperfections, accidental user scribing and proprietary device ink properties. The proposed segmentation approach relies on a robust estimation of the 4 corners of the print codes bounding box followed by creating a grid to separate individual blocks as illustrated by the lines in Figure 5. In short, the algorithm includes Otso's thresholding [14] operating on the saturation color component of the scanned image. A sequence of morphological operators are employed to estimate the bounding box of the print codes. The pixels along the edges of the bounding box are input to a least squares minimization algorithm providing robustness to boundary noise and to estimate the 4 corners required to create the grid. The resulting grid is robust to channel noise, internal scribing, coffee spills and geometric distortions. Auxiliary visual cues as employed in [2, 9] can be also used to improve the localization of the print codes.

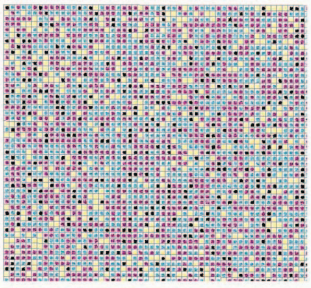

Fig. 5: Segmentation grid extracted from scanned print codes.

8. EXPERIMENTS

A set of inkjets and lasers printers (HPC4280, HPD6940, HPL1515, HPL2820) and scanners (HPC4280, HPL1120, HPS5590) are used with A4 size and standard office paper in all the experiments. The first set of experiments aims to observe the statistical properties of the printed and scanned data. Pages with blocks of one unique color are printed and the statistical moments (mean, variance, skewness and kurtosis) are extracted from each resulting color component from the observed printed and scanned pixels. The experiments indicate that the color statistics deviates slightly from a Gaussian distribution and the deviation is mostly dependent on the scanner optics. In these experiments, using the sample mean of the pixels inside of each square block (25 pixels), the kurtosis is kept around 20% of the value 3, and the skewness is less than 0.3. These values indicate that the distribution of the sample mean for the blocks can be approximated by a Gaussian pdf, where for perfect Gaussian pdf, the kurtosis would be 3 and skewness would be zero. For example, while printing magenta blocks, the scanned magenta component presented a kurtosis of 3.16 and skewness of -0.078. These values

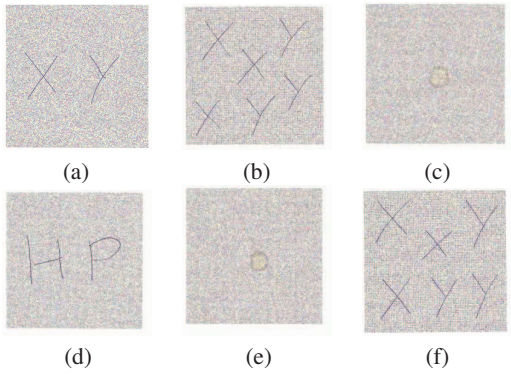

Fig. 6: Number and percentage of misclassified blocks (PMB) due to coffee spills and pen scribing and resulting bit errors after ECC: (a) 206 blocks, 0.36% PMB with BCH: 0 bits, (b) 556 blocks, 0.96% PMB with BCH: 9 bits, (c) 390 blocks, 0.68% PMB with BCH: 12 bits, (d) 324 blocks, 0.56% PMB with RS: 0 bits, (e) 341 blocks, 0.59% PMB with RS: 0 bits, (f) 560 blocks, 0.97% with RS: 44 bits.

may vary considerably depending on the devices, the color printed and the component scanned.

The second set of experiments aims to observe the robustness of the proposed classifier. Initially, synthetic channel errors (typical noise, optical and geometrical disturbances) are created to resemble real printing channel errors. A similar approach was used in [15] to validate channel models and analysis. For these typical channel errors, the segmentation and classification algorithms perform sufficiently well such that all block colors are detected without errors. It is not necessary to introduce ECC to deal with these errors since the classifier provides very high robustness to them. External synthetic distortions along with synthetic channel errors are introduced to observe the robustness of the classifier for these distortions: global and local blurring, pen scribing and small cropping. The pen scribing and cropping distortions introduce classification errors such that ECC algorithms are needed to help to deal with these external errors. The synthetic channel experiments indicate that the robustness of the ECC need to be proportional to the area of the external degradations on the document. Next, experiments with real channels are designed to introduce common external errors found in normal manipulation of documents, such as coffee spills, pen scribing and ink blurring due fingerprints. The ECC algorithms are designed to sustain these external distortions. The Figure 6 provides a few examples (from a large tested set) used to evaluate the system performance. The robust segmentation with the Bayesian classifier deals with the channel errors and the classifier takes the hard decision, while the ECC introduces at the print codes, before printing, the required redundancy to sustain the aforementioned external distortions.

9. CONCLUSIONS

The proposed novel statistic framework properly addresses the problem at hand and the performance was confirmed by a large set of experiments. The segmentation robustness and classification accuracy have been verified for a variety of devices. Currently, the system robustly embeds at least 900 bytes/in^2 with 20% of redundancy due to the ECC, resulting in an information payload amount of around 750 bytes/in^2, which is adequate for the Photoplus [7] and other applications. The print codes density can be increased by reducing the size of the blocks up to a certain limit imposed by segmentation issues and devices limitations. It may also be combined with a non payload indicia (NPI) approach [9] for color correction and localization, and it is envisioned that this hybrid technology is able to achieve higher than 3000 bytes/in^2 payload density with a very low bit error probability for demanding applications.

10. REFERENCES

[1] R. Villan; S. Voloshynovskiy; O. Koval; J. Vila; E. Topak; F. Deguillaume; Y. Rytsar and T. Pun, "Text data-hiding for digital and printed documents: theoretical and practical considerations," in *Proc. of SPIE*. SPIE, 2006, pp. 15–19.

[2] D. Parikh and G. Jancke, "Localization and segmentation of a 2d high capacity color barcode," in *IEEE Workshop on Applications of Computer Vision*, 2008, pp. 1–6.

[3] X. Liu; D. Doermann; H. Li, "A camera-based mobile data channel: capacity and analysis," in *Proceeding of the 16th ACM international conference on Multimedia*, October 2008, pp. 359 – 368.

[4] Songwen Pei; Guobo Li and Baifeng Wu, "Codec system design for continuous color barcode symbols," in *IEEE 8th International Conference on Computer and Information Technology Workshops*. IEEE, July 2008, vol. 8:11, pp. 539 – 544.

[5] D. Shaked; Z. Baharav; A. Levy; J. Yen and N. Saw, "Graphical indicia," in *Proc. IEEE International Conference on Image Processing*. IEEE, September 2003, vol. 1, pp. 485–488.

[6] N. Damera-Venkata and J. Yen, "Image barcodes," in *Proc. SPIE Color Imaging VIII: Processing, Hardcopy and Applications*. SPIE, January 2003, vol. 5008, pp. 493–503.

[7] R. Samadani and D. Mukherjee, "Photoplus: Auxiliary information for printed images based on distributed source coding," in *Visual Communications and Image Processing*, January 2008.

[8] S. Simske; J. Aronoff; M. Sturgill, "Spectral pre-compensation of printed security deterrents," in *The conference on optical security and counterfeit deterrence*, January 2008.

[9] S. Simske; J. Aronoff; M. Sturgill; G. Golodetz, "Security printing deterrents: A comparison of thermal inkjet, dry electrophotographic and liquid electrophotographic printing," in *J. Imaging Sci. Tech.*, October 2008, vol. 52:5, pp. 1–7.

[10] P. V. K. Borges; Joceli Mayer; Ebroul Izquierdo, "Document image processing for paper side communications," in *IEEE Transactions on Multimedia*. IEEE, November 2008, vol. 10:7, pp. 1277 – 1287.

[11] C. Bishop, "Pattern recognition and machine learning," in *Springer*, 2006.

[12] Rafael C. Gonzalez and Richard E. Woods, "Digital image processing," in *Prentice Hall*, 2007.

[13] Thomas M. Cover and Joy A. Thomas, "Elements of information theory," in *Wiley-Interscience*, 1991.

[14] N. Otsu, "A threshold selection method from gray-level histograms," in *IEEE Trans. Sys., Man., Cyber.*, 1979, vol. 9, p. 6266.

[15] P. V. K. Borges and Joceli Mayer, "Text luminance modulation for hardcopy watermarking," in *Signal Processing, Elsevier*, 2007, vol. 87:7, pp. 1754–1771.